Quantitative analysis of the element iron in aluminum alloy using LIBS

Zhao Xiaoxia[1], Luo Wenfeng[2], Wang Hongying[1], Yang Senlin[1], Zhu Haiyan[2], Li Shuli[1], Fu Fuxing[1], Li Yuanyuan[1]

(1. The Key Laboratory for Surface Engineering and Remanufacturing of Shaanxi Province, Institue of Applied Physics, Xi'an University, Xi'an 710065, China
2. School of Electronic Engineering, Xi'an University of Posts & Telecommunications, Xi'an 710121, China)

Abstract: In order to precisely analyze electron temperature and electron density of aluminum alloy, the Laser Induced Breakdown Spectroscopy was adopted. The second harmonic of a pulsed Nd:YAG laser (532 nm) has been used for the ablation of aluminum alloy E311 in air at atmospheric pressure and the laser-induced plasma characteristics were examined in detail. The electron density of 4.3×10^{16} cm^{-3} was inferred from the Stark broadening (0.12 nm) of the profile of Fe (I) 381.59 nm. In order to minimize relative errors in calculation of the electron temperature, an improved iterative Boltzmann plot method with eight iron lines (370.56, 386.55, 387.25, 426.05, 427.18, 430.79, 432.57, 440.48 nm) is used. Experimental results show that the electron temperature is 8 699 K with the regression coefficient of 0.999. The calibration curve for iron based on Fe (I) 404.58 nm was established using a set of six samples of standard aluminum alloy (E311, E312, E313, E314, E315, E316) and the detection limit was 0.077 9 wt%. The plasma was verified to be optically thin and in local thermodynamic equilibrium based on the experimental results.

Key words: atomic emission spectrum; laser-induced breakdown spectroscopy; plasmas
CLC number: O799 Document code: A Article ID: 1007-2276(2015)01-0096-06

基于 LIBS 技术铝合金中铁元素的定量分析

赵小侠[1],罗文峰[2],王红英[1],杨森林[1],朱海燕[2],李姝丽[1],付福兴[1],李院院[1]

(1. 西安文理学院 应用物理研究所 陕西省表面工程与再制造重点实验室,陕西 西安 710065;
2. 西安邮电大学 电子工程学院,陕西 西安 710121)

摘 要: 为了精确得到铝合金标样等离子体的电子温度和电子密度，实验采用激光诱导击穿光谱技术,利用 532 nm 调 Q Nd:YAG 激光器诱导产生铝合金 E311 等离子体。测量铁原子谱线(381.59 nm)的 Stark 展宽(0.12 nm)得到等离子体的电子密度是 4.3×10^{16} cm^{-3};基于铁原子谱线(370.56, 386.55, 387.25, 426.05, 427.18, 430.79, 432.57, 440.48 nm),利用迭代 Boltzmann 算法,得到回归系数为 0.999 时等离子体的电子温度是 8 699 K。基于铝合金标样(E311、E312、E313、E314、E315、E316)和铁原子谱

收稿日期: 2014-05-09; **修订日期:** 2014-06-14
基金项目: 陕西省教育厅科研计划项目(2013JK0607);西安市科技计划项目(CXY1443WL01,CX1289WL05,CXY1352WL02);国家自然科学基金(61401356)
作者简介: 赵小侠(1970-),女,副教授,博士,主要从事激光技术的应用研究。Email: 15029888059@126.com

线 404.58 nm,建立了铁元素的标准曲线,计算得到铁元素的探测限是 0.0779 wt%。等离子体特征参数表明铝合金等离子体满足光学薄和局部热力学平衡状态。

关键词:原子发射光谱; 激光诱导击穿光谱技术; 等离子体

0 Introduction

Nowadays laser-induced breakdown spectroscopy (LIBS) has become a well-known powerful tool for elemental analysis[1-2]. With this technique, a target is vaporized and ionized by a powerful laser pulse to form aluminous plasma when the breakdown threshold of the material is exceeded. By measuring the emission spectrum from the laser-induced plasma (LIP), qualitative and quantitative information about the sample's chemical composition can be obtained[3]. LIBS has gained extensive applications in steel industry[4], identification of alloys[5], and even extended to space exploration[6] with the capability of detecting all chemical elements in a sample without any preparation, of real-time response, and of close-contact or stand-off analysis of targets[2-3].

The interaction between the laser beam and the target is a complicated process, which is dependent not only on the properties of the laser (laser pulse temporal duration and shape, laser wavelength and energy), but also on the target material (mechanical, physical and chemical properties)[1-3]. There is no universal model to completely describe the process of laser-matter interaction and intensive investigation is still required.

In the present paper, the plasma parameters were studied based on Fe(I) lines in terms of their emission spectra, electron density and excitation temperature in air at atmospheric pressure. On one hand, the line intensity in the laser plasma emission spectra, which give information on the sample composition, depends on the total mass ablated by the laser. On the other hand, the amount of ablated matter, in its turn, depends on the absorption of the incident laser radiation affected by the plasma shielding, which is related to the electron density and temperature of the plasma[3,7]. Therefore, the knowledge of the plasma parameters is very important for understanding the laser-matter interaction processes. Furthermore, from the viewpoint of field-based and industrial applications, it is more practical to help improve the capability of the on-line sample analysis when performing experiments in air at atmospheric pressure. In the second set of the experiment, the optimum conditions for quantitative analysis of aluminum alloy have been studied and the calibration curve for iron at 404.58 nm was produced. The hypotheses of local thermal equilibrium (LTE) and optically thin plasma were also studied based on the experimental results.

1 Experiment

The LIBS system used in this work was shown in Fig. 1. A pulse from a Q-switched Nd: YAG laser (532 nm, 11 ns FWHM, 1 Hz, 80 mJ/pulse, SGR, Beamtech Optronics) was focused by a quartz lens (f =150 mm) onto the sample. The lens-to-sample distance was chosen to be slightly shorter than the focal length of the focusing lens in order to keep the emission stable. For all measurements, the sample was moved horizontally between shots with a **XYZ** stage to allow sampling from a fresh location. A bundle of five fibers(200 μm in diameter) collected the emission from the plasma spark at the right angle to the direction of the plasma expansion. The fibers were connected to a high-resolution (0.06-0.08 nm with 2 400-1 800 lines/mm) broadband spectrometer (AvanSpec-2048FT-5, Avantes, Netherlands) calibrated by the manufacturer using the standard light source. Each of the five fibers of the detection system connected to an individual component spectrometer (2 048 element linear CCD array) that covered a different segment of the 200-720 nm

spectral range. The AvanSpec-2048FT-5 detection system was triggered by the Q-switch of the laser with the delay time of 5 μs and integrated time of 2 ms.

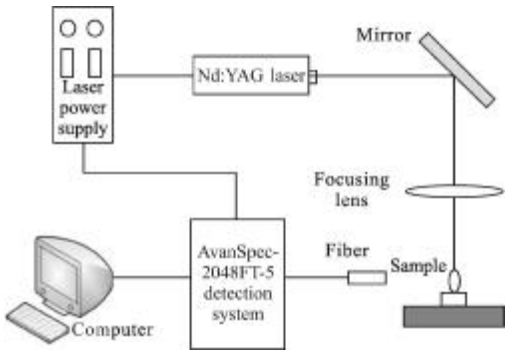

Fig.1 LIBS experimental setup

A set of six standard sample of aluminum alloy was bought from Shanghai Research Institute of Materials and the concentration of the element iron in each sample was given in Tab.1. All the experiments were performed in air at atmospheric pressure.

Tab.1 Iron concentration (wt%) in a set of standard aluminum alloy samples

Sample	E311	E312	E313	E314	E314	E316
Fe/wt%	0.454	1.21	0.908	1.61	1.87	0.115

2 Results and discussion

2.1 Plasma emission

Figure 2 showed a typical segment of the spectra of the 532-nm laser-induced aluminum alloy plasma. The spectrum consists of a continuum background and a number of neutral emission lines of the component species. At early plasma times, the signal is mostly dominated by the continuum emission which is attributed to the collisions of electrons with ions and atoms and the recombination of electrons with ions. As time progresses, continuum background diminishes while ionic and atomic emission lines become dominant[2]. To obtain the best signal background ratio (SBR) and to improve the line resolution, the delay time (5 μs), which is the time between the laser shot and the initiation of data acquisition, was chosen in our experiments. The assignment of these atomic lines shown by the arrows in Fig.2 was done using NIST database[8]. In our experiments, three neutral iron lines were used to determine the plasma temperature, while the Fe(I) 381.59nm emission line was used to calculate the electron number density in the plasma and the Fe(I) 404.58 nm was used to produce calibration curve for this line is less interference with other emission lines. The relevant transition parameters for the Boltzmann plot method and for the calculation of the electron density were found in[8].

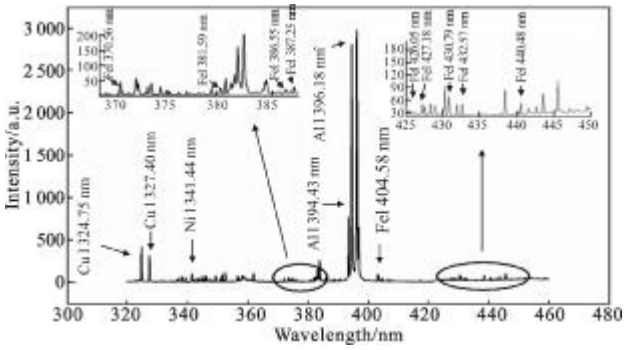

Fig.2 Segment of the LIBS spectra

2.2 Excitation temperature

Plasma descriptions start by trying to characterize the properties of the assembly of atoms, molecules, electrons and ions rather than the individual species. If thermodynamic equilibrium exists, then plasma properties, such as the relative populations of energy level and the distribution of the speed of the particles, can be described through the concept of temperature[2]. Under the LTE condition, the kinetic temperature and the excitation temperature are identical and can be determined from the Boltzmann diagram method. The population of the excited states follows the Boltzmann distribution and their relative spectral line intensity I_{mn} is given as[9-10]:

$$\ln\left(\frac{\lambda_{mn}I_{mn}}{hcg_mA_{mn}}\right)=-\frac{E_m}{kT_e}+\ln\left(\frac{N(T)}{U(T)}\right) \quad (1)$$

where λ_{mn} is the wavelength; A_{mn} is transition probability; g_m is the statistical weight of the upper level; h is the Plank constant, c is the speed of light in vacuum; E_m is the upper level energy, T_e is the electron

temperature; **k** is the Boltzmann constant; **U**(**T**) is the partition function and **N** (**T**) is the total number density of species, respectively. Plotting the expression on the left-hand side of the equation versus $\mathbf{E}_m$ yields a slope of $-1/(\mathbf{kT}_e)$ and the plasma temperature can be obtained.

To minimize the uncertainty in temperature determination, spectral lines should be chosen as far apart as possible in excitation energy. At the same time, the use of a series of lines from different excitation states of the same species can lead to greater precision of the plasma temperature determination[2]. In order to calculate the laser-ablated iron plasma temperature, an improved iterative Boltzmann plot method is used. First, eight neutral iron lines (370.56, 386.55, 387.25, 426.05, 427.18, 430.79, 432.57, 440.48 nm) are selected as potential candidates for the Boltzmann plot. After several iterations, a regression coefficient 0.999 is reached and the plasma temperature 8 669 K is inferred from the slope shown in Fig.3. Figure 4 also depicts the variations of the regression coefficient and the plasma temperature with the iteration number. The parameters of these lines are presented in Tab.2.

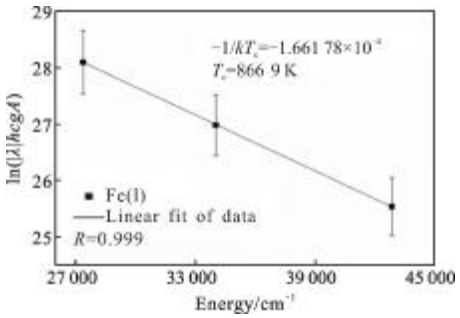

Fig.3 Boltzmann plot method for plasma temperature determination

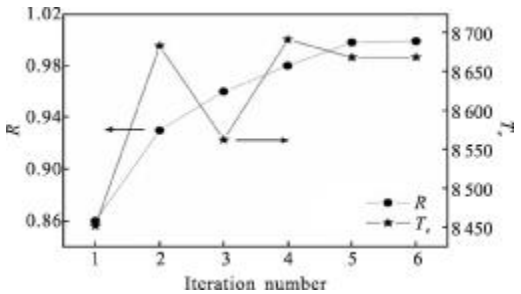

Fig.4 Variations of correlation coefficient and plasma temperature versus the iteration number

Tab.2 Physical parameters for Fe(I) transitions used for the deduction of the iron excitation temperature and electron density[8]

Species	Wave-length/nm	$\mathbf{E}_m$/cm^{-1}	$\mathbf{A}_{mn}$/10^7 s^{-1}	$\mathbf{g}_m$
Fe(I)	370.56	27 400	0.32	7
Fe(I)	381.59	38 175	11.20	7
Fe(I)	386.55	34 017	1.55	3
Fe(I)	387.25	33 801	1.05	5
Fe(I)	426.05	42 815	3.99	11
Fe(I)	427.18	35 379	2.28	11
Fe(I)	430.79	35 767	3.38	9
Fe(I)	432.57	36 079	5.16	7
Fe(I)	440.48	35 257	2.75	9

2.3 Electron density

Electron density is an important parameter that is used to describe the condition of the plasma environment and is crucial for establishing the equilibrium between different species. For the estimation for electron number density, the Stark broadened line profile of Fe(I) 381.59nm emission line was used. The Stark broadening is the result of interaction between emitting species and surrounding electrically charged species. Just as Barthelemy et al.[11] discussed, other broadening mechanisms were negligible under present experimental conditions. Considering the perturbations caused by ions is also negligible compared to electrons, the line FWHM $\Delta\lambda_{1/2}$(nm) can be simplified to equation (1)[11]

$$\Delta\lambda_{1/2}=2\omega\left(\frac{\mathbf{N}_e}{10^{16}}\right) \qquad (2)$$

where ω (nm) is the electron impact width parameter which can be found in [12]. Typical Stark broadened line profile is approximately Lorentzian and the experimental result was shown in figure 5 and fitted fairly well with a typical Lorentzian profile. The electron density was approximately 4.3×10^{16} cm^{-3}.

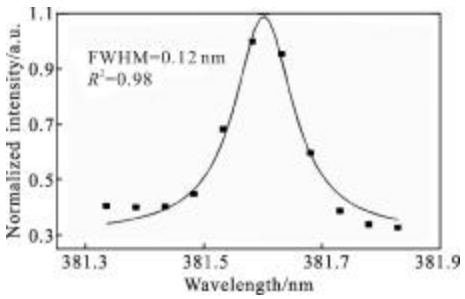

Fig.5 Stark broadened profile of Fe(I) 381.59 nm

2.4 LTE requirement and self-absorption analysis

To determine the electron temperature, the plasma must satisfy the equilibrium conditions, i.e. the plasma must hold a state of LTE during the observation window. In a LTE plasma, the collisional excitation and de-excitation processes must dominate radiative processes and this requires a minimum electron density. The lower limit for the electron density for which the plasma will be in LTE is[13]

$$\mathbf{N}_e(\mathrm{cm}^{-3}) \geqslant 1.4\times10^{14}\mathbf{T}^{1/2}(\mathrm{eV})[\Delta\mathbf{E}(\mathrm{eV})]^3 \quad (3)$$

where $\Delta\mathbf{E}$ is the energy difference between the upper and lower states. For the Fe (I) 307.56 nm line transition, $\Delta\mathbf{E}$= 3.34 eV, and the electron temperature observed was approximately 8 699 K. From equation (3), a minimum electron density of 4.52×10^{15} cm^{-3} was required for LTE to hold. As the requirement limit was much lower than the electron number density that we obtained, LTE was valid under present experimental condition.

When using the Boltzmann plot method to evaluate the electron temperature and using spectral line broadening to infer the electron number density, it is important to verify that the plasma is not optically thick. In optically thick plasmas, the radiation of an atom can be easily reabsorbed by other atoms of same element in energy level states[2-3]. This will cause a distortion in the spectral line. According to the Boltzmann law seen in Eq.(2), if the ratio of the intensities of the emission lines, whose upper energy levels are close to each other, is consistent with the ratio of their statistical weights, the line profiles will be considered to be free from self-absorption[14]. We took the transition 440.48 nm (upper level energy 4.37 eV) and 427.18 nm (upper level energy 4.38 eV) for example. The experimentally obtained transition probability ratio was 1.08 which was in agreement with the value 0.96 in the NIST database considering the experimental uncertainty. This indicated that the plasma was optically thin. Moreover, the lines we used neither showed a flat-toped profile nor showed a dip at the central frequency, further indicating the lines were free from self-absorption or self-reversal.

3 Calibration curve

The quantitative analysis is to relate the spectral line intensity of an element in the LIP to the concentration of that element in the target[7]. The calibration curve for element iron was shown in figure 6. The net emission intensity of Fe (I) 404.58 nm emission line, which was obtained by subtracting the background from the peak intensity of the line, was plotted as a function of the relative concentration of iron in aluminum alloy samples whose composition were shown in Tab.1, and the data were the average value of ten measurements. In the experiment, the laser beam was slightly defocused to avoid air breakdown by the higher laser intensity, and a better stability of the emission lines was obtained. At the same time, considering the spectrum was dominated by an intense continuum emission at early times following the plasma formation, a time delay (5 μs) was chosen in order to obtain a good compromise between the higher signal-to-background ratio and the emission intensity. The analyte line Fe (I) 404.58 nm was selected because it was free from spectral interference and its relative parameters(transition probability, upper level energy, etc.) are known in Ref [8]. As can be seen in Fig.6, a straight line with a correlation coefficient 0.97 can describe the curve. Experimental results show that the net spectral line intensities could be used for quantitative analysis without using complex methods if the experimental conditions are chosen properly.

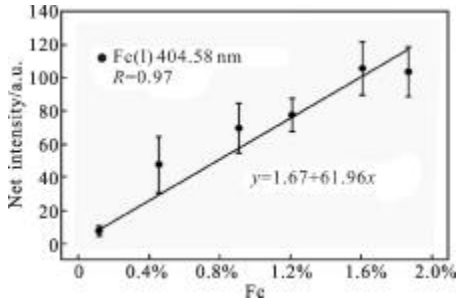

Fig.6 Calibration curve for Fe

The limit of detection (LOD) was determined by computing the slope (**m**) of the calibration curve and using the formula below[15]

$$LOD=\frac{2s_B}{m} \quad (4)$$

where s_B is the standard deviation of the background, which was determined from spectral regions that were located close to Fe (I) 404.58 nm. The detection limit determined in the present work was 0.077 9 wt%.

4 Conclusions

In this paper, laser ablation of an aluminum alloy using a 532 nm Nd:YAG laser was performed in air at atmospheric pressure. A time delay of 5 μs was used to gate off the early part of the signal in order to avoid the intense initial continuum emission and improve the signal-to-background ratio. The electron number density estimated from the Stark broadening profile of Fe(I) 381.59nm emission line was approximately $4.3\times10^{16}cm^{-3}$, which was much larger than the lower limit (McWhirter criterion) implying that LTE for the present experiment was valid. The electron temperature (8 699K) was inferred using an improved iterative Boltzmann plot method. The experimental transition probability ratio of Fe (I) 440.48nm to Fe (I) 427.18 was 1.08 which was in agreement with the value 0.96 in the NIST database within the experimental uncertainty indicating the laser-induced plasma was optically thin.

The calibration curve for element Fe based on Fe (I) 404.58 nm exhibited a good linear fit, and its LOD was 0.077 9wt%.

References:

[1] Luo W F, Sun Q B, Gao C X, et al. Plasma properties of 532 nm laser-ablated aluminum E414d target with direrent power densities [J]. Plasma Science and Technology, 2010, 12(4): 385-390.

[2] Cremers D A, Radziemski L J. Handbook of Laser-Induced Breakdown Spectroscopy [M]. Chichester: John Wiley & Sons, 2006: 156-159.

[3] Singh J P, Thakur S N. Laser-Induced Breakdown Spectroscopy [M]. Amsterdam: Elsevier, 2006, 205-209.

[4] Noll R, Bette H, Brysch A, et al. Laser-induced breakdown spectrometry-applications for production control and quality assurance in the steel industry[J]. Sturm V Spectrochim Acta B, 2001, 56(6): 637-640.

[5] Ma Demin, Ma Yanhua, Shu Rong, et al. Analysis of LIBS feasibility for in-situ dection of lunar soil components[J]. Infrared and Laser Engineering, 2007, 36 (5): 656 -658. (in Chinese)

[6] Lv Gang, Qi Hongxing, Pan Mingzhong, et al. Study on the laser induced breakdown spectroscopy overcoming the interfere from atmosphere [J]. Infrared and Laser Engineering, 2010, 40(4): 354-357. (in Chinese).

[7] Sabsabi M, Cielo P. Quantitative analysis of aluminum alloys by laser-induced breakdown spectroscopy and plasma characterization[J]. Appl Spectrosc, 1995, 49(4): 499-507.

[8] NIST Atomic Spectra Database Version: Atomic Spectroscopy [EB/OL]. http://www.nist.gov/pml/data/asd.cfm

[9] Rai S, Rai A K, Thakur S N. Identification of nitro-compounds with LIBS [J]. Appl Phys B, 2008, 91(3): 645-650.

[10] Aydin U, Roth P, Gehlen C D, et al. Spectral line selection for time-resolved investigations of laser-induced plasmas by an iterative Boltzmann plot method [J]. Spectrochim Acta Part B, 2008, 63(10): 1060-1065.

[11] Barthelemy O, Margot J, Chaker M, et al. Influence of the laser parameters on the space and time characteristics of an aluminum laser-induced plasma [J]. Spectrochim Acta Part B, 2005, 60(7): 905-914.

[12] Gehlen C D, Roth P, Aydin U, et al. Time-resolved investigations of laser-induced plasmas generated by nanosecond bursts in the millijoule burst energy regime [J]. Spectrochim Acta Part B, 2008, 63(10): 1072-1076.

[13] Abdellatif G, Imam H. Measurement of nutrients in green house soil with laser induced breakdown spectroscopy [J]. Spectrochim Acta Part B, 2002, 57(1): 1155-1165.

[14] Lu Zhigang, Zhan Renjun, Wang Xiaoyu, Characteristics of laser-induced plasma acoustic signal [J]. Infrared and Laser Engineering, 2014, 43(9): 2844-2849. (in Chinese)

[15] Long G L, Winefordner J D. Limit of detection a closer look at the IUPAC definition [J]. Anal Chem, 1983, 55(7):712-724.